

Melting Volume Variations of He³ at Very Low Temperatures

Louis Goldstein

University of California, Los Alamos Scientific Laboratory, Los Alamos, New Mexico 87544

(Received 1 December 1969; revised manuscript received 20 July 1970)

Liquid and solid volumes are calculated over the region of the melting anomaly for He³. Both phases are represented by theoretical models, and the volume variations are determined down to absolute zero. There is satisfactory agreement with measurements over the present experimental range. Although the melting-pressure curve is smooth, the solid volume at melting has a sharp cusp at its spin-ordering temperature. This feature should enable one to detect the process of spin ordering in the solid. The solid at melting expands with temperature decrease throughout its spin-ordering range. The volume change on adiabatic solidification of the liquid has also been obtained and should be useful in establishing a melting-pressure temperature scale based on the thermodynamic properties of melting He³ at very low temperature.

I. INTRODUCTION

In recent work¹ on melting He³, we gave a temperature scale of largely thermodynamic character down to 1 mK. The scale was based on the anomalous melting properties of this element, which extend from about 325 to 0.5 mK. However, in the application of this scale and in the design of cryogenic apparatus which is cooled by the adiabatic freezing of He³, it appears that further calculations of the volume variations at melting would be of interest. This is the main topic of the present paper.

The relationships between melting pressure and entropy, and melting pressure and temperature were obtained¹ from models for the liquid and solid which involve phenomenological parameters. These parametric functions can be refined as more accurate experimental data become available. Any lack of precision in the present calculations arises from the absence of isothermal compressibility data on liquid and solid He³ over the pressure and temperature ranges of interest. Assumed values of the compressibilities and their P and T dependence must thus be used along the melting line below the minimum. Other approximations may add to the uncertainty of the computed volume variations. Limitations of the melting pressure which enter in the discussion of volume changes have already been given.¹

The plan of the present paper is to consider the successive volume changes of the dense phases first over the melting temperatures and pressures where the solid is a nuclear paramagnet, and then over the very-low-temperature region where the solid is in the spin-ordering range. The difference between the liquid volume $V_{L,M}(T)$ and the solid volume $V_{S,M}(T)$ in equilibrium at melting defines the volume change $\Delta V_M(T)$. We then obtain the adiabatic volume change $\Delta V_M(S)$ which accompanies the freezing process at constant entropy S , and find it to be considerably larger than $\Delta V_M(T)$. Experi-

mental values of $\Delta V_M(S)$ should contribute to the establishment of a largely thermodynamic temperature standard at very low temperatures¹ and should aid in the design of He³ refrigerators which cool by the so-called Pomeranchuk effect.

II. VOLUME VARIATIONS OF LIQUID He³ AT MELTING; BOTH PHASES ARE PARAMAGNETIC

The molar-volume variation of the liquid at melting is given by

$$\begin{aligned} dV_{L,M} &= \left(\frac{\partial V_{L,M}}{\partial T} \right)_P dT + \left(\frac{\partial V_{L,M}}{\partial P} \right)_T dP_M \\ &= \left(\frac{\partial V_{L,M}}{\partial T} \right)_P dT - \chi_{L,M} V_{L,M} dP_M, \end{aligned} \quad (1)$$

where

$$\chi_{L,M} = - \frac{1}{V_{L,M}} \left(\frac{\partial V_{L,M}}{\partial P} \right)_T \quad (2)$$

is the isothermal compressibility coefficient of the liquid at melting. For the sake of simplicity we will drop the subscript M , since all properties refer to melting conditions. In our earlier work¹ we were not able to represent analytically the thermal properties of the liquid at melting from $T_{\min} \approx 326$ mK down to 5 mK, and had to calculate them numerically. An analytical description was approximated below 5 mK.

We use the thermodynamic relation

$$\left(\frac{\partial V_L}{\partial T} \right)_P = - \left(\frac{\partial S_L}{\partial P} \right)_T, \quad (3)$$

where $S_L(T, P)$ is the molar entropy of the liquid at melting, with the variable P referring to the melting pressure P_M . By virtue of the theory² of thermal excitations in liquid He³, we may write the entropy $S_L(T, P)$ as the sum of the spin (σ) and nonspin ($\nu\sigma$) entropies:

$$S_L(T, P) = S_{L,\sigma}(T, P) + S_{L,ns}(T, P). \quad (4)$$

Over the low-temperature range one has

$$S_{L,\sigma} > S_{L,ns} \quad (5a)$$

and at the lowest temperatures

$$S_{L,\sigma} \gg S_{L,ns}. \quad (5b)$$

While a formal representation of $S_{L,\sigma}(T, P)$ exists throughout the state surface of the liquid phase, the pressure dependence of $S_{L,ns}$ is only known qualitatively. One thus finds³

$$\left(\frac{\partial V_{L,\sigma}}{\partial T}\right)_P = -\left(\frac{\partial S_{L,\sigma}}{\partial P}\right)_T = \frac{C_{L,\sigma}(T)}{T_{0,L}(P)} \frac{dT_{0,L}}{dP}, \quad (6)$$

where $C_{L,\sigma}$ is the spin heat capacity of the liquid at melting, and $T_{0,L}(P)$ is the function giving the pressure dependence of the characteristic temperature of the spin system.² Since $dT_{0,L}/dP < 0$, we find that the partial derivative $(\partial V_{L,\sigma}/\partial T)_P < 0$, resulting in an anomalous spin expansion coefficient. By Eq. (6) the spin entropy increases on isothermal compression. However, the expansion coefficient arising from the nonspin degrees of freedom is expected to be positive. Hence, we have

$$\left(\frac{\partial V_L}{\partial T}\right)_P = \left(\frac{\partial V_{L,\sigma}}{\partial T}\right)_P + \left(\frac{\partial V_{L,ns}}{\partial T}\right)_P \geq \left(\frac{\partial V_{L,\sigma}}{\partial T}\right)_P, \quad (7)$$

and in the present calculations we must use a lower limit of this partial derivative. The calculated volume increase of the liquid at melting between T_μ , the temperature of the melting-pressure minimum, and some lower temperature T will always be larger than the actual volume increase. If we rewrite (1) as

$$dV_L = dV_L^{(T)} + dV_L^{(P)}, \quad (8)$$

we obtain, on integrating the first term on the right-hand side from T_μ to $T < T_\mu$,

$$V_L^{(T)}(T) - V_L^{(T)}(T_\mu) \leq V_{L,\sigma}(T) - V_{L,\sigma}(T_\mu). \quad (9)$$

Integrating the term $dV_L^{(P)}$, one has with (1)

$$V_L^{(P)}(P) - V_L^{(P)}(P_\mu) = (-) \int_{P_\mu}^P \chi_L V_L dP. \quad (10)$$

Since the connection between T and P , at melting, is unique, we may rewrite (10) as

$$V_L^{(P)}(T) - V_L^{(P)}(T_\mu) = (-) \int_{T_\mu}^T \chi_L(T') V_L(T') \frac{dP}{dT'} dT'. \quad (11)$$

It is seen that this volume change involves an integration over the unknown volume $V_L(T')$. Since the liquid- and solid-volume changes are small, various approximation procedures suggest themselves.

These may be refined to come as close as desired to an exact evaluation of (11), as far as $V_L(T)$ is concerned. Our main problem is obtaining information about $\chi_L(T)$. Grilly⁴ has been experimentally investigating this function for both liquid and solid He³ down to about 0.30 K. Solid-He³ compressibilities were deduced by Adams and his collaborators⁵ from pressure measurements along a series of isochores of the solid. Equation-of-state data on the liquid down to about 1.0 K were used by Sherman and Edeskuty⁶ to derive liquid compressibilities. Liquid compressibilities at melting were also deduced by Mills, Grilly, and Sydoriak⁷ from their data on the melting properties of He³ down to about T_μ . More recently, Straty and Adams⁸ obtained liquid and solid compressibilities at melting from their equation-of-state data at temperatures $T \geq 0.35$ K.

At the higher temperatures⁶ it appears that variations in χ_L arise mainly from the effects of pressure. This suggests that the compressibilities at a given pressure will be about the same on the two branches of the melting-pressure curve, below and above its vertex. A recent measurement⁹ of the liquid compressibility at 31.5 atm at about 40 mK was in good agreement with the higher-temperature compressibility⁶ at about the same pressure.

The present volume calculations will be made with the following assumptions: (a) An averaged constant value $\langle \chi_L \rangle$ will be used over the small temperature and pressure ranges considered here. (b) The experimentally determined volumes will be bracketed by two sets of compressibility values. This same procedure will be followed in subsequent calculations of the solid volumes.

As a starting (α) approximation we may write instead of (1)

$$dV^{(\alpha)}(T) = \left(\frac{\partial V_{L,\sigma}}{\partial T}\right)_P dT - \langle \chi_L \rangle V_L(T_\mu) dP(T). \quad (12)$$

Integrating between T_μ and $T < T_\mu$, we find

$$V_L^{(\alpha)}(T) = V_L(T_\mu) \{1 - \langle \chi_L \rangle [P(T) - P(T_\mu)]\} + \int_{T_\mu}^T \left(\frac{\partial V_{L,\sigma}}{\partial T}\right)_P dT. \quad (13)$$

It is convenient to introduce the notation

$$k_L(T, T_r) = \langle \chi_L \rangle [P(T) - P(T_r)], \quad (14a)$$

$$v_L(T, T_r) = \int_{T_r}^T \left(\frac{\partial V_{L,\sigma}}{\partial T}\right)_P dT, \quad (14b)$$

T_r being a reference temperature. In the (α) approximation, the liquid volume at melting is then

$$V_L^{(\alpha)}(T) = V_L(T_\mu) [1 - k_L(T, T_\mu)] + v_L(T, T_\mu), \quad (15)$$

which can be refined over small temperature intervals to yield the (β) approximation. Let $T_1, T_2, \dots, T_j, \dots$, be a series of temperatures such that $T_1 > T_2 > \dots > T_j > T_{j+1} > \dots$. Then, at $T < T_j$, we have

$$dV_L^{(\beta)}(T) = \left(\frac{\partial V_{L,\sigma}}{\partial T} \right)_P dT - \langle \chi_L \rangle V_L^{(\beta)}(T_j) dP(T). \quad (16)$$

Integrating between T_j and T_{j+1} , we obtain

$$V_L^{(\beta)}(T_{j+1}) = V_L^{(\beta)}(T_j) [1 - k_L(T_{j+1}, T_j)] + v_L(T_{j+1}, T_j), \quad (17)$$

where k_L and v_L are defined by (14). In this (β) approximation, the constancy of $V_L(T)$ on the right-hand side of (16) is assumed over the small interval (T_{j+1}, T_j) only, instead of over the whole interval (T, T_μ) , as in (12). The (β) approximation can be made to approach the actual correct limit of $V_L(T)$ as closely as one desires, on narrowing the interval (T_{j+1}, T_j) .

A somewhat different calculation of $V_L(T)$ at $T < T_\mu$ involves rewriting (1) as

$$d \ln [V_L(T)] = [V_L(T)]^{-1} \left(\frac{\partial V_{L,\sigma}}{\partial T} \right)_P dT - \langle \chi_L \rangle dP(T). \quad (18)$$

With $V_L(T)$ replaced by $V_L(T_\mu)$ on the right-hand side, we obtain on integration

$$V_L^{(\alpha')} (T) = V_L(T_\mu) \exp \{ -k_L(T, T_\mu) + [V_L(T_\mu)]^{-1} v_L(T, T_\mu) \}, \quad (19)$$

the (α') approximation to $V_L(T)$. Since the exponent is quite small, (19) reduces to $V_L^{(\alpha)}(T)$.

Stepwise integration over intervals (T_{j+1}, T_j) gives the (β') approximation:

$$V_L^{(\beta')} (T_{j+1}) = V_L^{(\beta')} (T_j) \exp \{ -k_L(T_{j+1}, T_j) + [V_L^{(\beta')} (T_j)]^{-1} v_L(T_{j+1}, T_j) \}, \quad (20)$$

which reduces to $V_L^{(\beta)}(T_{j+1})$ [Eq. (17)].

Near T_μ , (18) may be rewritten as

$$[V_L(T_\mu)]^{-1} \left(\frac{dV_L}{dT} \right) \approx [V_L(T_\mu)]^{-1} \left(\frac{\partial V_{L,\sigma}}{\partial T} \right)_P - \langle \chi_L \rangle \frac{dP}{dT}. \quad (21)$$

The two terms on the right-hand side are of opposite sign below T_μ . This is true even if $(\partial V_{L,\sigma}/\partial T)_P$ were to be included in the first term. As shown earlier^{10,11} the liquid volume at melting exhibits a maximum just below T_μ on the basis of reasonable values of $\langle \chi_L \rangle$. Below the temperature of this maximum, $V_L(T)$ decreases monotonically with decreasing temperatures.

It is simpler to define $V_L(T)$ at $T < 5$ mK, where

the spin heat capacity $C_{L,\sigma}$ and spin entropy $S_{L,\sigma}$ become linear in T . One has

$$C_{L,\sigma}/R \approx \gamma_{L,\sigma}(0)T \quad (T \text{ small}),$$

$$\gamma_{L,\sigma}(0) \approx (\frac{3}{2} \ln 2) / T_{0,L}(P - P(0)) \approx 4.23 \times 10^{-3} / \text{mK}, \quad (22)$$

$T_{0,L}(P(0))$ being the characteristic temperature of the spin system of the liquid at the limit $P(T \rightarrow 0)$. One thus finds

$$\left(\frac{\partial V_{L,\sigma}}{\partial T} \right)_P = \gamma_{L,\sigma}(0)RT \{ d \ln [T_{0,L}(P)/dP] \}, \quad (T < 5 \text{ mK}). \quad (23)$$

Here $d \ln (T_{0,L}/dP)$ is estimated from magnetic susceptibilities¹² to be about $(-)$ $1.1 \times 10^{-2}/\text{atm}$, with $P_M(0)$ taken to be about 34 atm.¹

At $T < 5$ mK, dV_L/dT can be approximated analytically. On the right-hand side of (18) $(\partial V_{L,\sigma}/\partial T)_P$ can be replaced by (23). Then, in the second compressional term in (18), one has

$$\left(\frac{dP}{dT} \right)_{T < 5 \text{ mK}} \approx (R/\langle \Delta V \rangle) \{ \gamma_L T - [S_s(T)/R] \}, \quad (24)$$

where

$$S_L/R \approx \gamma_L T, \quad (T \text{ small}) \quad (25)$$

$$S_s/R = \ln 2 - 3 \sum_{n=0}^{\infty} (-)^n (a_n/n+2) x^{n+2}, \quad (26)$$

$$x = \langle J \rangle / kT, \quad \langle J \rangle / k \approx 0.7 \text{ mK},$$

as discussed earlier¹ assuming an antiferromagnetic model for the solid.¹³ The limiting value γ_L in Eq. (25) has already been considered.¹³ The average values of the melting-volume change $\langle \Delta V \rangle$ and the compressibility $\langle \chi_L \rangle$ complete the list of parameters entering into dV_L/dT .

We now describe the various approximation schemes at low temperatures. Let T_r be a starting low temperature of 5 mK. In the (α) approximation we obtain an expression for $V_L^{(\alpha)}(T)$ similar to (15), where T_r replaces T_μ . With (24)–(26), we find

$$k_L(T, T_r) = \langle \chi_L \rangle (R/\langle \Delta V \rangle) \left\{ (T_r - T) \ln 2 - \frac{1}{2} \gamma_L (T_r^2 - T^2) + 3 \left(\frac{\langle J \rangle}{k} \right) \sum_{n=0}^{\infty} (-)^n \frac{a_n}{(n+1)(n+2)} \left(\frac{\langle J \rangle}{kT_r} \right)^{n+1} \times \left[1 - \left(\frac{T_r}{T} \right)^{n+1} \right] \right\}, \quad (27)$$

$$v_L(T, T_r) = \int_{T_r}^T \left(\frac{\partial V_{L,\sigma}}{\partial T} \right)_P dT = \frac{1}{2} R \gamma_{L,\sigma}(0) \frac{d \ln T_{0,L}}{dP} (T^2 - T_r^2). \quad (28)$$

Hence, the initial (α) approximation for $V_L(T)$ at $T < T_r$, with the help of (15), is

$$V_L^{(\alpha)}(T, T_r) = V_L^{(\alpha)}(T_r)[1 - k_L(T, T_r)] + v_L(T, T_r). \quad (29)$$

Here, $k_L(T, T_r)$ and $v_L(T, T_r)$ refer to (27) and (28).

Similarly the (β) approximations are derived from (17) by way of (27) and (28) to obtain, respectively,

$$k_L(T_{j+1}, T_j) = k_L(T_{j+1}, T_r) - k_L(T_j, T_r), \quad (30)$$

$$v_L(T_{j+1}, T_j) = v_L(T_{j+1}, T_r) - v_L(T_j, T_r), \quad (31)$$

where all temperatures $T_j \leq T_r = 5$ mK.

Again the (α') approximation to $V_L(T)$ at low temperatures results from (19) on replacing $V_L(T_\mu)$ by $V_L^{(\alpha')}(T_r)$, $k_L(T, T_\mu)$ and $v_L(T, T_\mu)$ by $k_L(T, T_r)$ and $v_L(T, T_r)$ [Eqs. (27) and (28)]. Similarly, the (β') approximation results from (20) using (30) and (31) for $k_L(T_{j+1}, T_j)$ and $v_L(T_{j+1}, T_j)$.

III. MELTING-VOLUME VARIATIONS OF PARAMAGNETIC SOLID He³ AT LOW TEMPERATURES

The calculation of the volume change of solid He³ at melting follows that for the liquid and yields

$$\begin{aligned} dV_s(T, P) &= \left(\frac{\partial V_s}{\partial T} \right)_P dT + \left(\frac{\partial V_s}{\partial P} \right)_T dP \\ &= \left(\frac{\partial V_s}{\partial T} \right)_P dT - \chi_s V_s dP, \end{aligned} \quad (32)$$

$$\begin{aligned} V_s^{(\alpha)}(T, T_\mu) &= V_s(T_\mu) \{1 - \langle \chi_s \rangle [P(T) - P(T_\mu)]\} \\ &\quad + \int_{T_\mu}^T \left(\frac{\partial V_s}{\partial T} \right)_P dT \\ &= V_s(T_\mu) [1 - k_s(T, T_\mu)] + v_s(T, T_\mu), \end{aligned} \quad (33)$$

where the subscript L is replaced by s . The total change of V_s below T_μ is less than about 3%.

We will use two sets of compressibilities to calculate $V_s(T)$. In the first set, the liquid and solid compressibilities are taken to be equal. This is compatible with early measurements⁴ of χ_L and χ_s above T_μ . As a second set, we will use solid compressibilities calculated from equation-of-state data,⁸ which indicate that at about 1.0 K the solid at melting has a larger compressibility than the liquid in equilibrium with it.

The entropy of the solid can be represented¹ as the sum of entropies from spin excitations $S_{x,s}$ and phonon excitations $S_{\phi,s}$. From earlier work^{13,14} on the exchange-coupled model of solid He³, we have

$$\left(\frac{\partial P}{\partial T} \right)_{V_s} = \left(\frac{\partial S_s}{\partial V_s} \right)_T = \left(\frac{\partial S_{x,s}}{\partial V_s} \right)_T + \left(\frac{\partial S_{\phi,s}}{\partial V_s} \right)_T$$

$$= V_s^{-1} (\Gamma_x C_{x,s} + \Gamma_\phi C_{\phi,s}). \quad (34)$$

Here, the C 's denote the component heat capacities. The entropy $S_{x,s}$ is represented¹ by a high-temperature expansion in ascending powers of the ratio $[J(V_s)/kT]$, where $J(V_s)$ is a temperature-independent parameter describing the numerical value of the exchange energy of an antiferromagnet.¹⁵ The volume derivatives of the entropies involve derivatives of $J(V_s)$ and $\Theta(V_s)$, the latter being the Debye temperature. In addition to the Grueneisen parameter

$$\Gamma_\phi = - \frac{\partial \ln[\Theta(V_s)]}{\partial \ln V_s}, \quad (35a)$$

we define¹⁶ the corresponding quantity

$$\Gamma_x = - \frac{\partial \ln |J(V_s)|}{\partial \ln V_s}, \quad (35b)$$

relating to the exchange system. It should be noted that a similar parameter involving pressure derivatives has been given by us earlier¹³ in connection with the calculations of the isobaric expansion coefficient of the solid along the melting line. Values of $J(V_s)$ and Γ_x have been obtained by the Florida workers, who were the first to show spin ordering in the bcc solid at very low temperatures.^{16,17} Values of Γ_ϕ have been deduced from heat-capacity data¹⁸ and from equation-of-state data.⁸ With (34) and the thermodynamic relation

$$\left(\frac{\partial V}{\partial T} \right)_P = \chi V \left(\frac{\partial P}{\partial T} \right)_V, \quad (36)$$

the total temperature derivative of the solid volume at melting becomes

$$\frac{dV_s}{dT} = \chi_s \left(\Gamma_x C_{x,s} + \Gamma_\phi C_{\phi,s} - V_s \frac{dP}{dT} \right). \quad (37)$$

The exchange system is anomalous to the extent that $(\partial S_{x,s}/\partial V_s)_T < 0$, which requires, by (34), that $\Gamma_x < 0$, in agreement with the observations.^{9,16,17} The normal behavior of the lattice imposes $\Gamma_\phi > 0$. The contrasting behaviors of the spin system and the lattice were shown to impose a minimum upon the isobars and isochores of solid He³. The locus of this minimum was given earlier^{13,14} and was determined recently by Panczyk and Adams.¹⁷ At $T \geq 200$ – 230 mK, depending on values assigned to $J(V_s)$, Γ_x , Θ , and Γ_ϕ , the positive phonon term ($\Gamma_\phi C_{\phi,s}$) outweighs the negative exchange term ($\Gamma_x C_{x,s}$) on the right-hand side of (37). Hence, dV_s/dT can vanish only at $T > T_\mu$ where $dP/dT > 0$. One finds thus that the solid volume at melting has a maximum just beyond T_μ as conjectured earlier.^{10,11}

In calculating the volume variations at $T < T_\mu$, the starting (α) approximation, [Eq. (33)], can be improved in a way similar to the case of the liquid. Through stepwise integration one obtains the (β) approximation:

$$V_s^{(\beta)}(T_{j+1}) = V_s^{(\beta)}(T_j)[1 - k_s(T_{j+1}, T_j)] + v_s(T_{j+1}, T_j), \quad T_{j+1} < T_j, \quad (38)$$

where

$$k_s(T_{j+1}, T_j) = \langle \chi_s \rangle [P(T_{j+1}) - P(T_j)], \quad (39a)$$

$$v_s(T_{j+1}, T_j) = \int_{T_j}^{T_{j+1}} \left(\frac{\partial V_s}{\partial T} \right)_P dT, \quad (39b)$$

and $\langle \chi_s \rangle$ is assumed to be constant. The (α') and (β') approximations to $V_s(T)$ follow by analogy to the liquid at melting.

In contrast to $P(T)$ and dP/dT , which cannot be given in analytical form from T_μ to about 5 mK because the liquid entropy has no analytical representation there, the partial derivative $(\partial V_s/\partial T)_P$, represented by the first two terms on the right-hand side of (37) can be described analytically for $T < T_\mu$. With $C_{x,s}$ and $C_{\varphi,s}$ calculated earlier,^{13,14} (37) yields the explicit formula

$$\left(\frac{\partial V_s}{\partial T} \right)_P = R \langle \chi_s \rangle \left[3\Gamma_x \sum_{n=0} (-)^n a_n \left(\frac{\langle J \rangle}{kT} \right)^{n+2} + \frac{12\pi^4}{5} \Gamma_\varphi \left(\frac{T}{\Theta} \right)^3 \right], \quad (40)$$

which is valid down to the spin-ordering temperature T_0 . The two terms inside the brackets are of opposite sign, since $\Gamma_x < 0$ and $\Gamma_\varphi > 0$; the coefficients a_n are known up to a_8 , $\langle J \rangle$ denotes the average exchange energy as in (26). According to (37), dV_s/dT is positive, so $V_s(T)$ increases monotonically from $T_r \sim 5$ mK to its maximum just above T_μ . As indicated earlier $(\partial V_s/\partial T)_P$ becomes negative below about 200–230 mK, but the compressional term $(-\langle \chi_s \rangle) V_s(dP/dT)$ in (37) is always positive over the range (T_r, T_μ) causing $V_s(T)$ to increase.

It is instructive to look at dV_L/dT and dV_s/dT from $T = 5$ mK to T_μ . As we have seen, dP/dT approaches zero at T_μ , while the positive derivative dV_L/dT also approaches zero. The maximum in V_L occurs at about 302 mK and arises from compensation of the negative spin term $(\partial V_{L,\sigma}/\partial T)_P$ by the positive compressional term $-\langle \chi_L \rangle V_L(dP/dT)$. Below this maximum the compressional term increases rapidly and becomes some five times larger than the spin term at 200 mK. The ratio increases to over 200 at 7 mK, where $-(dP/dT)$ or $(-\langle \chi_L \rangle) \times (dP/dT)$ reaches its maximum. At very low temperatures, variations of $V_L(T)$ are defined only by

the compressional term

$$\frac{dV_L}{dT} \simeq (-\langle \chi_L \rangle) V_L \frac{dP}{dT} \quad (T \text{ small}) . \quad (41)$$

Both $V_L(T)$ and $P(T)$ have inflection points^{1,13} near 7 mK which cause a minimum in $V_L(T)$ at very low temperatures, since $(-)(d^2P/dT^2)$ is positive below the temperature of the inflection point.

The volume of the solid at melting also has an inflection point near that for $P(T)$, but on its high-temperature side. The inflection points of V_L and V_s arise because $(-\langle \chi_L \rangle) V_L(dP/dT)$ and $(-\langle \chi_s \rangle) V_s \times (dP/dT)$ dominate over the terms $(\partial V_{L,\sigma}/\partial T)_P$ and $(\partial V_s/\partial T)_P$ in the total derivatives dV_L/dT and dV_s/dT . However, near the spin-ordering temperature and below, $(\partial V_s/\partial T)_P$ becomes larger than the compressional term.

It is convenient to write down explicitly the small-volume term $v_s(T, T_\mu)$ on the right-hand side of (33), or $v_s(T_{j+1}, T_j)$ on the right-hand side of (38). With

$$v_s(T_{j+1}, T_j) = v_s(T_{j+1}, T_\mu) - v_s(T_j, T_\mu), \quad (42)$$

one finds, using (40),

$$v_s(T, T_\mu) = R \langle \chi_s \rangle \left\{ 3(-\Gamma_x) \frac{\langle J \rangle}{k} \sum_{n=0} (-)^n \frac{a_n}{n+1} \left(\frac{\langle J \rangle}{kT_\mu} \right)^{n+1} \times \left[\left(\frac{T_\mu}{T} \right)^{n+1} - 1 \right] + \frac{3\pi^4}{5} \Gamma_\varphi \frac{T_\mu^4}{\Theta^3} \left[\left(\frac{T}{T_\mu} \right)^4 - 1 \right] \right\}. \quad (43)$$

Remembering that $-\Gamma_x$ is a positive number, we see that the exchange system causes the volume to expand on cooling, while the second phonon term inside the braces causes it to contract.

Below 5 mK, Eqs. (24)–(26) can be used in (37) to obtain the analytical form of dV_s/dT . The k_s function in Eq. (38) takes on an analytical expression through (27) where $\langle \chi_L \rangle$ is replaced by $\langle \chi_s \rangle$, and T and T_μ are replaced by T_{j+1} and T_j .

We have thus formulated the liquid- and solid-volume variations from T_μ down to the spin-ordering temperature within the limitations mentioned earlier. As in our treatment¹ of $P(T)$, we have neglected any critical behavior of the solid near the spin-ordering temperature.

In Fig. 1 we give the calculated liquid and solid volumes $V_L^{(\beta)}$ and $V_s^{(\beta)}$ from 5 mK to T_μ . The upper and lower liquid-volume curves result from using $\langle \chi_L \rangle = 5.2 \times 10^{-3}/\text{atm}$ and $\langle \chi_L \rangle = 5.5 \times 10^{-3}/\text{atm}$, respectively. The solid volumes correspond to compressibilities of $5.5 \times 10^{-3}/\text{atm}$, upper curve, and $5.94 \times 10^{-3}/\text{atm}$, lower curve. Experimental volumes⁹ are shown as the open circles, and their extrapolated values as the closed circles. The calculated volume curves bracket the data, with volumes calculated from the smaller liquid compress-

TABLE I. Isothermal melting-volume changes $[V_L(T) - V_s(T)]$ at low temperatures.

T (mK)	$\Delta V(T)^a$ cm ³ /mole	$\Delta V(T)^b$
300	1.203	1.201
280	1.207	1.204
260	1.211	1.208
240	1.216	1.215
220	1.221	1.223
200	1.227	1.229
180	1.233	1.237
160	1.240	1.247
140	1.248	1.254
120	1.256	1.264
100	1.266	1.272
90	1.271	1.274
80	1.276	1.276
70	1.286	1.278
60	1.287	1.279
50	1.289	1.276
45	1.295	1.276
40	1.298	1.276
35	1.300	1.275
30	1.303	1.275 ^c
25	1.306	1.274 ^c
20	1.309	1.273 ^c
15	1.311	1.272 ^c
10	1.314	
5	1.315	

^aCalculated with V_L and V_s obtained with the averaged compressibilities of 5.2×10^{-3} and 5.94×10^{-3} /atm, respectively.

^bDeduced in Ref. 9 from separate determinations of $V_L(T)$ and $V_s(T)$.

^cExtrapolated data included in Ref. 9.

ibility and the larger solid compressibility being close to the data points.

The calculated volume curves reproduce the melting-volume data⁹ to within about 0.1% or to within about 3×10^{-2} cm³/mole. Hence, the isothermal volume change at melting

$$\Delta V(T) = V_L(T) - V_s(T), \quad (44)$$

which is of the order 1 cm³/mole, is given to within 3%. The largest deviations between the experimental and calculated values of $\Delta V(T)$ are expected to occur at the lower temperatures, where the calculated volumes differ most from the data.

Listed in Table I are the calculated values of $\Delta V(T)$ and those deduced by Scribner, Panczyk, and Adams⁹ from their separate determinations of the volumes $V_L(T)$ and $V_s(T)$. The calculated ΔV values become larger than those resulting from the experimental melting volumes as the temperature decreases, but they tend to level off at the lowest temperatures where variations of V_L and V_s become very small. As Fig. 1 suggests, the volume can change very little below 5 mK. This change for both phases is found to be about $(13-16) \times 10^{-3}$

cm³/mole between 5 mK and $T_0 \approx 2$ mK. The zero of dV_s/dT occurs at about 2.10 mK, where $V_s(T)$ has a minimum. Any volume changes in the limited temperature range below this minimum would be extremely small and of mostly theoretical interest.

IV. MELTING-VOLUME VARIATIONS OF He³ AT VERY LOW TEMPERATURES: SOLID IS IN SPIN-ORDERING RANGE

The temperature derivative of the melting-pressure at $T < T_0$ is¹

$$\frac{dP_m}{dT} = \frac{R}{\langle \Delta V \rangle} \left\{ \left(\gamma_L T - \frac{S_+(T_0)}{R \ln 2} [\ln(2 \cosh y) - xy] \right) \right\}. \quad (45)$$

The term linear in T on the right-hand side is the entropy of the liquid as given in Eq. (24). The second term is the entropy of the antiferromagnetic solid. $S_+(T_0)$ is the entropy of the paramagnetic solid at T_0 which is assumed to be identical with that of its antiferromagnetic modification at the transition temperature.¹ The quantities x and y are defined by

$$x = \tanh y = \sigma(T)/\sigma_0, \quad y = x/\tau; \quad \tau = T/T_0, \quad (46)$$

$\sigma(T)$ and σ_0 being the magnetic moments per sublattice at T and absolute zero, respectively.

The partial derivative $(\partial V_L/\partial T)_P$ is still given by Eq. (23). The compressional part of dV_L/dT is now

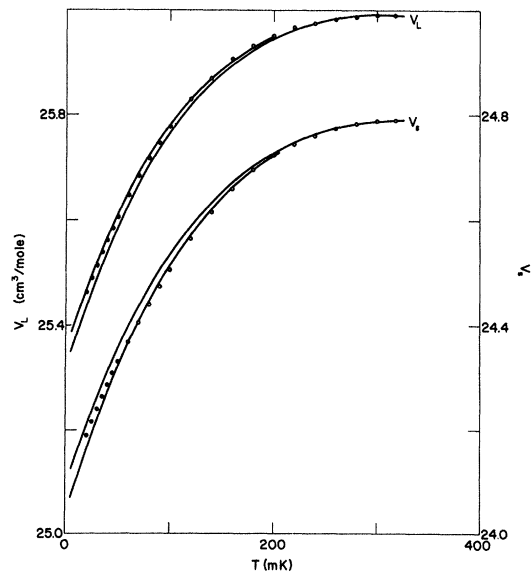


FIG. 1. Calculated liquid V_L and solid volumes V_s at melting, (cm³/mole), as a function of the temperature (mK). The upper and lower curves refer, respectively, to the smaller and larger isothermal compressibility parameters at melting. The circles represent the data of Ref. 9.

$$\frac{dV_{L-}^{(P)}}{dT} = (-) \langle \chi_L \rangle V_L(T_0) \frac{dP_-}{dT}, \quad (47)$$

with dP_-/dT given by (45). One finds, as above,

$$V_{L-}^{(\alpha)}(T) = V_L(T_0)[1 - k_{L-}(T, T_0)] + v_{L-}(T, T_0), \quad (48)$$

with

$$k_{L-} = \langle \chi_L \rangle [P_-(T) - P_-(T_0)], \quad (49)$$

$$v_{L-}(T, T_0) = \int_{T_0}^T \left(\frac{\partial V_{L-}}{\partial T} \right)_P dT \\ = \frac{1}{2} \gamma_{L,\sigma}(0) \frac{d \ln T_{0,L}}{dP} R(T^2 - T_0^2), \quad T < T_0 \quad (50)$$

as in (28) above. This v_{L-} term is quite small. We gave earlier¹ the expression of $[P_-(T) - P(T_0)]$ as

$$P_-(T) - P(T_0) = (RT_0 / \langle \Delta V \rangle) \left\{ -\frac{1}{2} \gamma_L T_0 (1 - \tau^2) \right. \\ \left. + [S_+(T_0) / R \ln 2] [(1 - \tau) \ln 2 \right. \\ \left. + \frac{1}{2} x^2 + \frac{1}{2} \tau \ln(1 - x^2)] \right\}. \quad (51)$$

The liquid volume $V_{L-}(T)$ decreases only by about $2 \times 10^{-3} \text{ cm}^3/\text{mole}$ between T_0 and the absolute zero. Actually $V_L(T)$ has an extremely shallow minimum at a somewhat higher temperature than the very low temperature maximum of $P_-(T)$ at about 0.5 mK as discussed earlier.¹ Stated in other terms, dV_{L-}/dT vanishes at a temperature somewhat higher than dP_-/dT . This is caused by the negative $(\partial V_{L-}/\partial T)_P$ becoming larger than the positive compressional term [Eq. (47)], that is, the melting volume of the liquid expands at the approaches of the absolute zero. This result is of theoretical significance only, since volume variations even down to T_0 cannot be measured at the present time. However, volume variations in liquid He considerably smaller than $2 \times 10^{-3} \text{ cm}^3/\text{mole}$ are measurable at higher temperatures according to my colleagues, Kerr and Sherman.

Omitting the very small phonon term in the spin-ordering range of the solid, one has with (37)

$$\frac{dV_{s-}}{dT} = \langle \chi_s \rangle \left(\Gamma_x C_{s-} - V_{s-} \frac{dP_-}{dT} \right), \quad (52)$$

where Γ_x is defined through (35b) and C_{s-} is the heat capacity of the spin-ordering solid in the absence of the very small phonon heat capacity. We saw above, that $V_s(T)$ developed a very shallow minimum slightly above T_0 and increased at the approaches of T_0 . Below the maximum¹ of $P_M(T)$ at about 0.5 mK, the two terms on the right-hand side of (52) are both negative. Hence, solid He³ at melting is anomalous from 2.10 mK down to

absolute zero.

As discussed earlier,¹ the asymptotic molecular-field-theory model gives a λ -type discontinuity in the heat capacity at the transition temperature T_0 . Since $\Gamma_x < 0$, dV_s/dT is seen to develop an inverted λ discontinuity which, with (37) and (52), is

$$\Delta \frac{dV_s}{dT} = \left(\frac{dV_s}{dT} \right)_+ - \left(\frac{dV_s}{dT} \right)_- = \langle \chi_s \rangle (\Gamma_x) (-\Delta C) \\ = \Delta \left(\frac{\partial V_s}{\partial T} \right)_P > 0, \quad (53)$$

where

$$\Delta C = C_{s+}(T_0) - C_{s-}(T_0), \quad (54)$$

and the isothermal compressibility is assumed to be continuous. To this approximation, the discontinuity of the total volume derivative dV_s/dT at T_0 reduces to that of the partial temperature derivative $(\partial V_s/\partial T)_P$ of the isobar $P \rightarrow P(T_0)$ at its end point on the melting-pressure line at T_0 . This same type of discontinuity occurs in $(\partial V_s/\partial T)_P$ along the locus $T_0(P)$, where the solid is bcc. The discontinuity $\Delta(\partial V_s/\partial T)_P$ is expected to decrease slowly along the transition line $T_0(P)$ up to the bcc-hcp transition. At the spin-ordering temperature, only the derivative of the melting pressure dP/dT shows a break,¹ whereas V_s itself has such a cusp according to Eq. (53).

With $(-\Delta C) = 0.364R$, $|\Gamma_x| \sim 16.4$,¹⁶ and the values of $\langle \chi_s \rangle$ indicated above, the discontinuity $\Delta(dV_s/dT)$ is about $(2.7-2.9) \times 10^{-3} \text{ cm}^3/\text{mole mK}$. The more recent value of $|\Gamma_x|$ is somewhat larger¹⁷ and $\Delta(dV_s/dT)$ may have to be increased by 5-8%. Discontinuities in the slope of the isochores of the solid at the transition line are related to the temperature coefficients

$$\Delta \left(\frac{\partial p}{\partial T} \right)_{V_s} = \left(\frac{|\Gamma_x|}{V_s} \right) (-\Delta C) \quad (55)$$

by Eq. (53). Near melting, with $|\Gamma_x| \sim 17$, $V_s \sim 24 \text{ cm}^3/\text{mole}$, this amounts to about (0.027 atm/mK) , the temperature derivatives being larger at T_0 than at T_0 , as with the volume derivatives [Eq. (53)]. Both discontinuities (53) and (55) are quite large and should result in sharp breaks in the isobars and isochores. If working temperatures of $T \geq 1.5 \text{ mK}$ are attainable, the angular character of the isochores may help to locate the spin-ordering transition at least near the melting curve. A sensitive technique developed by Adams and his collaborators^{16,17} for measuring isochores might be applied to the present case. Clearly, magnetic measurements across the spin-ordering temperatures would supply additional information. Even isochores with relatively poor temperature resolution should yield values close to $\Delta C = (-0.364)R$,

through Eq. (55).

On integration of dV_s/dT [Eq. (52)] one finds

$$V_s(T_0) - V_s(T) = \langle \chi_s \rangle \left(\Gamma_x [U(T_0) - U(T)] - \int_T^{T_0} V_{s-}(T) \frac{dP_-}{dT} dT \right), \quad (56)$$

where¹

$$U(T_0) - U(T) = \frac{1}{2} [S_+(T_0)/R \ln 2] RT_0 [\sigma(T)/\sigma_0]^2 \quad (57)$$

is the internal energy difference of the model between T_0 and T . At these very low temperatures, the (α) approximation should be sufficient to yield with fair accuracy the second term inside the large parentheses on the right-hand side of (56). Hence, we find

$$V_{s-}(T) - V_s(T_0) = \langle \chi_s \rangle \{ |\Gamma_x| [U(T_0) - U(T)] - V_s(T_0) [P_-(T) - P(T_0)] \}, \quad (58)$$

where $P_-(T) - P(T_0)$ is given by (51). With

$$U(T_0) - U(0) = \frac{1}{2} RT_0 \frac{S_+(T_0)}{R \ln 2},$$

the present treatment gives¹

$$\lim_{T \rightarrow 0} P_-(T) - P(T_0) = \frac{RT_0}{\langle \Delta V \rangle} \left[\frac{S_+(T_0)}{R} \left(1 - \frac{1}{2 \ln 2} \right) - \frac{1}{2} \gamma_L T_0 \right]. \quad (59)$$

The expression giving the limit value $[V_{s-}(T \rightarrow 0) - V_s(T_0)]$ can be written as

$$V_{s-}(0) - V_s(T_0) = RT_0 \langle \chi_s \rangle \left\{ \frac{1}{2} |\Gamma_x| \frac{S_+(T_0)}{R \ln 2} - \frac{V_s(T_0)}{\langle \Delta V \rangle} \left[\frac{S_+(T_0)}{R \ln 2} \left(1 - \frac{1}{2 \ln 2} \right) - \frac{1}{2} \gamma_L T_0 \right] \right\}. \quad (60)$$

Using the smaller value of $\langle \chi_s \rangle$, $\langle \Delta V \rangle \sim 1.20 \text{ cm}^3/\text{mole}$, $|\Gamma_x| = 16.4$, $T_0 \approx 2.04 \text{ mK}$, and $V_s(T_0) \sim 24.111 \text{ cm}^3/\text{mole}$, one finds that the solid volume at absolute zero is larger than at T_0 by about $2.7 \times 10^{-3} \text{ cm}^3/\text{mole}$. One finds this difference to increase to about $2.9 \times 10^{-3} \text{ cm}^3/\text{mole}$ using the larger solid compressibility which gives $V_s(T_0) \sim 24.059 \text{ cm}^3/\text{mole}$. An additional small increase of this volume difference would result by using the larger value of $|\Gamma_x|$ indicated above. These volume differences are essentially reached at $T/T_0 \sim \frac{1}{2}$ or about 1 mK. Values of V_L computed from the smaller compressibility are 25.3868, 25.3712, and 25.3690 cm^3/mole at $T = 5 \text{ mK}$, T_0 , and $T = 0$, respectively. The larger compressibility V_s values are, respectively,

24.0716, 24.0592, and 24.0620 cm^3/mole . Corresponding values of $\Delta V(T)$ result by subtraction.

Over the range explored so far⁹ the calculated liquid and solid volumes at melting are in fair agreement with the experimental volumes. In principle, verification could be extended even lower. In Table I the isothermal volume changes at melting $\Delta V(T)$, resulting from $V_L(T)$ and $V_s(T)$, are in poorer agreement with experimental volumes.⁹ The calculated ΔV values become larger than the experimental ones toward the low-temperature end of the experimental range. By introducing the calculated $\Delta V(T)$ values into the melting-pressure derivatives, with the improved $J(V)$ function¹⁷ we can determine the entropy of the solid at very low temperature. This yields a new approximation to dP/dT and $P(T)$. The latter can be reintroduced into new calculations of $V_L(T)$, $V_s(T)$, and $\Delta V(T)$. These can now be used to arrive at improved functions of dP/dT and $P(T)$. Or a major iterative procedure can be followed for improving successively the melting properties until, hopefully, convergence results. In the absence of new theoretical or experimental liquid entropies, and liquid and solid compressibilities, such a procedure is not warranted at the present time.¹⁹ Any improvements in the numerical values of the melting properties would probably involve only minor corrections. However, in the future when investigations yield improved parameters, the iteration procedure may be useful in recalculating the various melting properties of He³. A temperature scale¹ based on the thermodynamic properties of melting He³ would improve accordingly.

Our final calculations involve the volume changes which accompany the adiabatic freezing of He³. In this process the initial state is an all-liquid sample of coordinates $(T_i, P(T_i), V_L(T_i), S_L(T_i))$, at melting, and the final state is an all-solid sample of coordinates $(T_f, P(T_f), V_s(T_f), S_s(T_f))$. The volume change is

$$\Delta V(S) = V_L(T_i) - V_s(T_f), \quad S_s(T_f) = S_L(T_i). \quad (61)$$

The constant-entropy volume changes should be accessible to accurate measurement and should broaden the foundation of a temperature scale¹ of thermodynamic character.

The entropies of liquid and solid He³ become equal at three points on the melting curve: $(T_\mu, P(T_\mu))$, $(T_{f,\mu}, P(T_{f,\mu}))$, and in the limit of absolute zero. Again¹ $T_{f,\mu}$ is the intersection of the liquid- and solid-entropy curves at very low temperature. The entropy degeneracies impose the following degeneracies on melting-volume changes during adiabatic and isobaric-isothermal freezing:

$$\Delta V(T = T_\mu) = \Delta V(S_L(T_\mu) = S_s(T_\mu)),$$

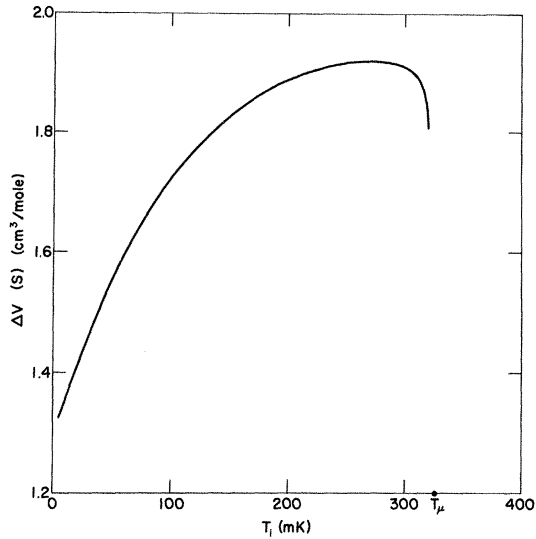


FIG. 2. Volume changes (cm^3/mole) on adiabatic freezing of an initial all-liquid sample at melting, as a function of the initial temperature T_i (mK) of the liquid. For the invariant-entropy values [$S_L(T_i) = S_s(T_f)$] and the final temperatures T_f see Ref. 1.

$$\Delta V(T = T_{f, \mu}) = \Delta V(S_L(T_{f, \mu}) = S_s(T_{f, \mu})), \quad (62)$$

$$\Delta V(T = 0) = \Delta V(S_L = S_s \rightarrow 0).$$

The melting anomaly of He^3 requires¹

$$\Delta P(S_L(T_i) = S_s(T_f)) \geq 0, \quad T_f \leq T_i \quad (63)$$

as well as

$$\Delta V(S_L(T_i) = S_s(T_f)) \geq \Delta V(T_i = T_f = T), \quad T_f \leq T_i. \quad (64)$$

From T_μ to $T_{f, \mu}$, $\Delta V(S)$ increases from $\Delta V(T_\mu)$ to

a maximum at about the same initial temperature T_i of the adiabatic freezing process where $\Delta P(S)$ was shown¹ to display a maximum. Instead of using T_i or T_f to denote the initial and final temperatures associated with the complete adiabatic freezing process, the entropy $S = S_L(T_i) = S_s(T_f)$ can be used as an independent variable of $\Delta V(S)$. We have used this notation¹ to display variations of $\Delta P(S)$ in the freezing process. Beyond its maximum, $\Delta V(S)$ decreases toward its second limit $\Delta V(T_{f, \mu})$ at the end of the melting anomaly, which is estimated to be about $1.307 \text{ cm}^3/\text{mole}$. Within our present treatment this is also the melting-volume difference at absolute zero.

In Fig. 2 the graph of the $\Delta V(S(T_i))$ function is given for values of T_i between 320 and 5 mK. These volume changes accompany the adiabatic freezing of an initial all-liquid sample at melting to an all-solid sample at melting. The values of $S_L(T_i) = S_s(T_f)$ have been given elsewhere.¹

Hopefully, experimental investigations of melting He^3 will be refined and extended to lower temperatures and will aid in establishing a temperature standard of thermodynamic character. The present calculations should prove useful to those who carry out the experiments.

ACKNOWLEDGMENTS

My sincere thanks go to Mrs. J. E. Powers for most of the numerical work. My colleagues and friends in the experimental group, Dr. R. L. Mills, Dr. E. C. Kerr, and Dr. R. H. Sherman have cooperated through patient discussions of several problems considered in this paper. I have also benefited from friendly discussions on melting He^3 with Dr. E. D. Adams during a brief visit to Los Alamos.

¹L. Goldstein, Phys. Rev. **188**, 349 (1969).

²L. Goldstein, Phys. Rev. **96**, 1455 (1954); **112** 1465, (1958); **112**, 1483 (1958).

³L. Goldstein, Phys. Rev. **133**, A52 (1964).

⁴E. R. Grilly (private communication).

⁵E. D. Adams, G. C. Straty, and E. L. Wall, Phys. Rev. Letters **15**, 549 (1965).

⁶R. H. Sherman and F. J. Edeskuty, Ann. Phys. (N. Y.) **9**, 522 (1960).

⁷R. L. Mills, E. R. Grilly, and S. G. Sydorik, Ann. Phys. (N. Y.) **12**, 41 (1961).

⁸G. C. Straty and E. D. Adams, Phys. Rev. **169**, 232 (1968).

⁹R. A. Scribner, M. F. Panczyk, and E. D. Adams, J. Low Temp. Phys. **1**, 313 (1969). These workers have independently discussed the use of melting He^3 as a thermometric system. Actually, the idea of melting- He^3 thermometry was put forward by E. D. Adams as early as 1967 at the discussions at the Gordon Research Conference, Dynamics of Quantum Solids and Liquids, Crystal Mountain, Washington, 1967 (unpublished).

¹⁰L. Goldstein, Ann. Phys. (N. Y.) **16**, 205 (1961).

¹¹L. Goldstein and R. L. Mills, Phys. Rev. **128**, 2479 (1962).

¹²A. L. Thomson, H. Meyer, and E. D. Adams, Phys. Rev. **128**, 509 (1962).

¹³L. Goldstein, Phys. Rev. **159**, 120 (1967).

¹⁴L. Goldstein, Phys. Rev. **176**, 311 (1968).

¹⁵The antiferromagnetic character of solid He^3 has been established recently by two independent groups of investigators through measurements on the nuclear paramagnetic susceptibility of this solid at temperature as low as 5–6 mK. See J. R. Sites, D. D. Osheroff, R. C. Richardson, and D. M. Lee, Phys. Rev. Letters **23**, 835 (1969); W. P. Kirk, E. B. Osgood, and M. Garber, Phys. Rev. Letters **23**, 833 (1969). See also the very much higher temperature experiments of P. B. Pipes and W. M. Fairbank, Phys. Rev. Letters **23**, 520 (1969).

¹⁶M. F. Panczyk, R. A. Scribner, G. C. Straty, and E. D. Adams, Phys. Rev. Letters **19**, 1102 (1967).

¹⁷M. F. Panczyk and E. D. Adams, Phys. Rev. **187**, 321 (1969).

¹⁸H. H. Sample and C. A. Swenson, Phys. Rev. **158**,

188 (1967).

¹⁹Since from about 15–20 mK down to about 1.0 mK, $S_L \ll S_g$, the new larger $\Delta V(T)$ values would justify the use of a corrective factor of about 0.92–0.93 to our dP/dT values (see Ref. 1). Also, the same factor is to be used to the melting-pressure difference $P(T)$

– $P(T_r)$, with $T < T_r$ and $T_r \sim 15$ –20 mK. The larger $\Delta V(T)$ values of Ref. 9 have been used in the recent work of R. T. Johnson, O. G. Symko, and J. C. Wheatley, Phys. Rev. Letters **23**, 1017 (1969). These workers also consider the possibility of using melting He³ as a thermometer. See in this connection Ref. 9.

PHYSICAL REVIEW A

VOLUME 2, NUMBER 5

NOVEMBER 1970

Diffusion Coefficient of He₂(³Σ_u⁺)[†]

M. A. Gusinow and R. A. Gerber

Sandia Laboratories, Albuquerque, New Mexico 87115

(Received 18 May 1970)

The diffusion coefficient for the helium metastable molecule in a 300 °K helium afterglow has been measured. The experimental technique is that of particle counting instead of the usual method of optical absorption. The value obtained was $D_M P_0 = 361 \pm 34 \text{ cm}^2 \text{ sec}^{-1} \text{ Torr}$.

In 1955 Phelps¹ published a definitive study of the afterglow properties of atomic and molecular helium. The results were obtained by measuring the time-varying optical absorption of the various metastables.

We report here late-afterglow measurements of the diffusion coefficient for an excited neutral particle which we have assumed to be the helium molecular metastable, He₂(³Σ_u⁺). The sampling apparatus consisted of a quadrupole mass spectrometer (length = 5 cm) viewing along the axis of a cylindrical discharge tube. The tube had a characteristic diffusion length $\Lambda = 0.178$ cm. The ion detector was a Bendix channeltron which was directly in line with the plasma sampling aperture. The signal from the detector consisted of individual pulses which were counted by a multichannel analyzer operating in the multiscaling mode. With the mass spectrometer set for complete ion instability, i. e., zero ion transmission, the channeltron registered a time-varying background signal that we interpret as consisting of three components: (a) uv photons, (b) atomic metastables, and (c) molecular metastables.² At relatively late times in the afterglow, the decay of the background had the appearance of a linear process, i. e., it was linear on a semi-logarithmic plot. We interpret this linear process as the diffusive decay of He₂(³Σ_u⁺). Figure 1 illustrates the late-time behavior of the background. The early-time background is probably a combination of He(2³S) and uv radiation from the plasma and did not decay exponentially. The very early flux is so large that there is unquestionably saturation of both the detector and the counting system. The electron density at the time when one can clearly distinguish the diffusive decay of He₂(³Σ_u⁺) is about 10^3 – 10^4 cm^{-3} .

The vacuum system had a base vacuum of 10^{-9}

Torr. The helium was purified by a cataphoretic discharge before admission to the plasma vessel. In the afterglow the ratio of impurity atoms to helium atoms was $\sim 10^{-10}$. During the several days of experimentation the impurity level tended to rise (undoubtedly because of emission from the electrodes). We found that the most sensitive way to observe the relative impurity level was to monitor the afterglow decay of He₂^{*}. He₂^{*} reacts quite strongly with just about all impurities. (As an aside we must mention the following: When a leak to air was purposely introduced, the background was effectively reduced to zero. This behavior is consistent with our interpretation of the background signal as being due to metastables).

Figure 1 presents some sample data of the late-time decay at several pressures. These plots are illustrative of an "impurity-free" system. When the impurity level was raised to 10^{-7} – 10^{-8} of the helium filling, it was not possible to clearly distinguish the exponential decay of the molecular metastable.

Figure 2 is a plot of the determined value of $D_M P_0$ versus P_0 , where $P_0 = P(273 \text{ °K}/300 \text{ °K})$. Here D_M is the molecular metastable diffusion coefficient and P is the pressure. The afterglow was isothermal at 300 °K as verified by measurements of the diffusion coefficient of He₂^{*}. There are two reasons why this value of $D_M P_0$ is not that of He(2³S): (a) The accepted value³ for He(2³S) is $445 \text{ cm}^2 \text{ sec}^{-1} \text{ Torr}$. (b) The value of $D_M P_0$ is independent of P_0 .

The average value of the $D_M P_0$ values shown in Fig. 2 is $361 \pm 34 (\pm 9.4\%) \text{ cm}^2 \text{ sec}^{-1} \text{ Torr}$, where the uncertainty represents the probable error. This value of $D_M P_0$ is significantly larger than the value $283 \pm 45 (\pm 16\%) \text{ cm}^2 \text{ sec}^{-1} \text{ Torr}$, reported by Phelps,¹ where the uncertainty represents the scatter in his data. However, it should also be